# Highly Efficient Ligands for Dihydrofolate Reductase from *Cryptosporidium hominis* and *Toxoplasma gondii* Inspired by Structural Analysis

Phillip M. Pelphrey,[†,‡] Veljko M. Popov,[†,‡] Tammy M. Joska,[§] Jennifer M. Beierlein,[#] Erin S. D. Bolstad,[#] Yale A. Fillingham,[‡] Dennis L. Wright,[||,#,*] and Amy C. Anderson[#,*]

*Department of Chemistry, Dartmouth College, Hanover, New Hampshire 03755, Department of Biochemistry, Dartmouth Medical School, Hanover, New Hampshire 03755, Department of Chemistry, University of Connecticut, Storrs, Connecticut 06269, and Department of Pharmaceutical Sciences, University of Connecticut, Storrs, Connecticut 06269*

*Received August 25, 2006*

The search for effective therapeutics for cryptosporidiosis and toxoplasmosis has led to the discovery of novel inhibitors of dihydrofolate reductase (DHFR) that possess high ligand efficiency: compounds with high potency and low molecular weight. Detailed analysis of the crystal structure of dihydrofolate reductase-thymidylate synthase from *Cryptosporidium hominis* and a homology model of DHFR from *Toxoplasma gondii* inspired the synthesis of a new series of compounds with a propargyl-based linker between a substituted 2,4-diaminopyrimidine and a trimethoxyphenyl ring. An enantiomerically pure compound in this series exhibits $IC_{50}$ values of 38 and 1 nM against *C. hominis* and *T. gondii* DHFR, respectively. Improvements of 368-fold or 5714-fold (*C. hominis* and *T. gondii*) relative to trimethoprim were generated by synthesizing just 14 new analogues and by adding only a total of 52 Da to the mass of the parent compound, creating an efficient ligand as an excellent candidate for further study.

## Introduction

*Cryptosporidium* and *Toxoplasma* are apicomplexan parasitic protozoa that cause severe disease in the population worldwide. Cryptosporidiosis, caused by *C. hominis*, is characterized by wasting disease and most often affects immune-compromised patients, the elderly, and day-care children, although very large outbreaks have occurred in otherwise healthy populations.[1] There is no effective therapy for cryptosporidiosis. Toxoplasmosis, when transmitted congenitally as *T. gondii*, can cause neonatal death and when transmitted through ingestion of contaminated meat or water, can cause fever and sore throat, or cerebral inflammation in immune-compromised patients.[1] Both of these parasitic protozoa have been classified as Category B biodefense agents.

Dihydrofolate reductase (DHFR[a]) has been a validated drug target for treatment of protozoal infections for decades. Occurring as a bifunctional protein with thymidylate synthase (DHFR−TS) in the apicomplexan protozoa, DHFR utilizes the cofactor NADPH to catalyze the reduction of dihydrofolate to tetrahydrofolate, thereby performing a key reaction in the sole *de novo* synthesis of deoxythymidine monophosphate (dTMP). The overall fold of DHFR is widely conserved throughout evolution; however, there are several residue differences in the active sites of different species that make achieving selectivity for the pathogenic form of the enzyme possible. The DHFR inhibitor pyrimethamine (**1**, Figure 1) has been effectively used to treat toxoplasmosis[2] as well as malaria,[3] caused by another apicomplexan parasite, *Plasmodium*. However, many patients have had severe reactions to pyrimethamine, limiting its efficacy.

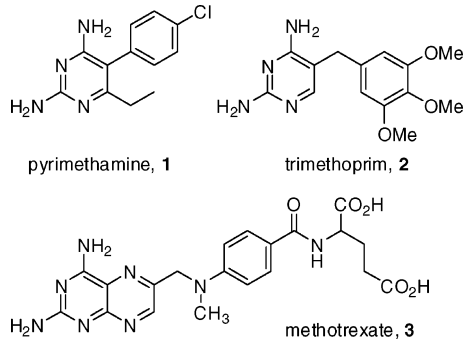


**Figure 1.**

Trimethoprim (**2**, TMP, Figure 1) has been used effectively in the clinic as an antibacterial agent since the 1960s. It possesses excellent drug-like characteristics including relatively low molecular weight (MW = 290). However, it exhibits high affinity for only a small subset of species of DHFR from pathogenic organisms such as *Escherichia coli*, thus limiting its widespread application. TMP exhibits only moderate *in vitro* potency against DHFR from *C. hominis* (ChDHFR) ($IC_{50}$ = 14 $\mu$M)[4] and *T. gondii* (TgDHFR) ($IC_{50}$ = 8 $\mu$M).[5,6] Although TMP may not be clinically useful against these DHFR targets, it may serve as a lead compound in the design of higher potency DHFR inhibitors.

It is often appreciated that during the lead optimization process, increases in potency correlate with increases in molecular weight. However, the additional molecular weight frequently represents a liability as it compromises the drug-like properties of the lead.[7,8] The necessary compromise between increasing molecular weight and increasing affinity can be examined quantitatively with the concept of ligand efficiency.[9,10] Ligand efficiency is defined as the overall binding energy per

* To whom correspondence should be addressed. Mailing address: Dept. of Pharmaceutical Sciences, University of Connecticut, 69 N. Eagleville Rd., Storrs, CT 06269. Phone (D.L.W.): (860) 486-1556, (A.C.A.): (860) 486-6145. Fax: (860) 486-6857. E-mail: Dennis.Wright@uconn.edu, Amy.Anderson@uconn.edu.

‡ Department of Chemistry, Dartmouth College.

§ Department of Biochemistry, Dartmouth Medical School.

|| Department of Chemistry, University of Connecticut.

# Department of Pharmaceutical Sciences, University of Connecticut.

† These authors contributed equally.

[a] Abbreviations: DHFR, dihydrofolate reductase; DHFR−TS, dihydrofolate reductase-thymidylate synthase; dTMP, deoxythymidine monophosphate; ChDHFR, dihydrofolate reductase from *Cryptosporidium hominis*; TgDHFR, dihydrofolate reductase from *Toxoplasma gondii*; TMP, trimethoprim; MTX, methotrexate; *p*ABA, *para*-aminobenzoic acid; NADPH, nicotinamide adenine dinucleotide phosphate.

10.1021/jm061027h CCC: $37.00 
Published on Web 02/02/2007

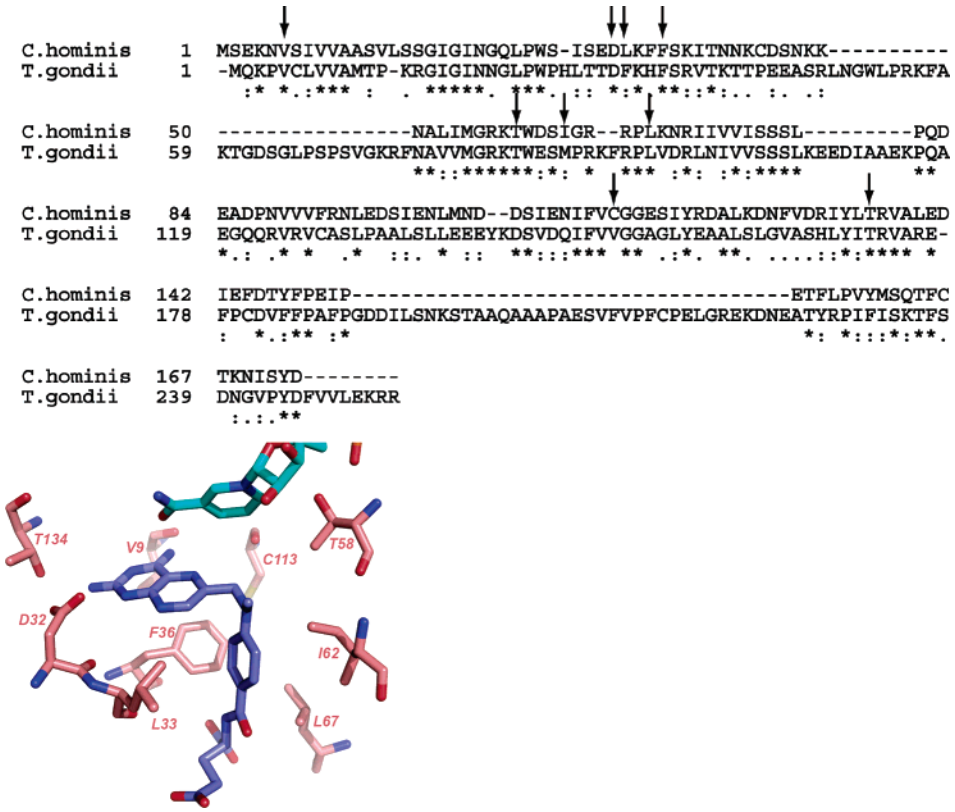


**Figure 2.** (a) Sequence alignment of ChDHFR (PDB code: AAB00163) and TgDHFR (PDB code: XP665866). Arrows indicate residues located in the active site. (b) MTX modeled in the ChDHFR active site.

**Scheme 1**[a]

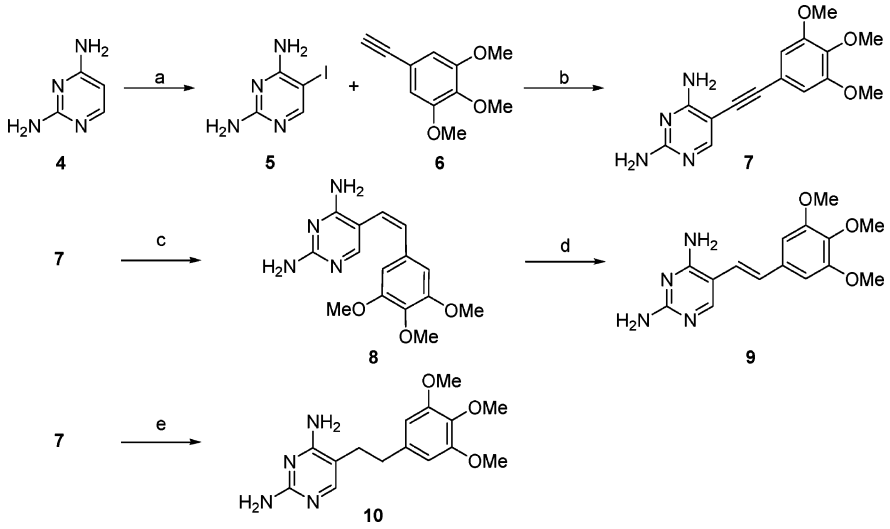


[a] Reagents and conditions: (a) ICl, MeOH, 25 °C, 15 h, then 1N NaOH, 25 °C, 2 h (80%); (b) $Pd(PPh_3)_2Cl_2$, CuI, $Et_3N$, DMF, 100 °C, 2 h (90%); (c) 5% Pd/C, EtOH, 45 psi $H_2$, 25 °C, 5 h (33%, 81% borsm); (d) $I_2$, THF, 25 °C, 30 min (80%); (e) 10% Pd/C, MeOH, 50 psi $H_2$, 25 °C, 10 h (87%).

nonhydrogen atom;[9] higher ligand efficiency defines a superior compound. Interestingly, although methotrexate (**3**, MTX, Figure 1) is a much more potent compound ($IC_{50}$ values against ChDHFR and TgDHFR are 23 nM and 14 nM, respectively) than TMP, it has the same ligand efficiency as TMP, implying that the increased potency is largely dependent on the increased molecular weight rather than a more optimal positioning of pharmacophoric elements. It should be possible to design a highly efficient ligand for DHFR that possesses the potency of MTX while maintaining low molecular weight.

Accurate computational prediction of protein−ligand interactions is a great advantage in the ligand design process since it allows the chemist more confidence in the selection of compounds slated for synthesis. Establishing reliable docking procedures with known compounds allows more accurate predictions of new compounds. In previous work,[11] we docked 30 compounds into the crystal structure of ChDHFR and established high (72.9%) correlations between the docking scores and biological activity. Including protein flexibility in the docking method and assessing an ensemble of the lowest-energy docked complexes was critical to achieving this correlation between calculated and experimental values.

In this manuscript, we present a novel, low molecular weight scaffold for DHFR inhibitors that exhibits nanomolar potency

**Table 1.** Inhibitory Potency of DHFR Ligands ($IC_{50}$ Values in $\mu$M)

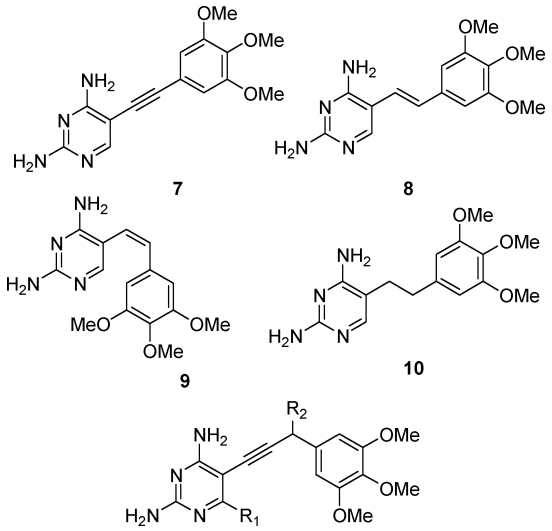


| compound | $R_1$ | $R_2$ | ChDHFR | TgDHFR | docking score vs ChDHFR[a] |
|---|---|---|---|---|---|
| TMP | N/A | N/A | 14 | 8 | 5.94 |
| **7** | N/A | N/A | >1000 | N/D | - |
| **8** | N/A | N/A | >1000 | N/D | - |
| **9** | N/A | N/A | >1000 | N/D | - |
| **10** | N/A | N/A | >1000 | 90.2 ± 19.1 | - |
| **14** | H | H | 86.1 ± 7.3 | 21.7 ± 3.3 | 6.98 |
| **16** | $CH_3$ | H | 10.2 ± 0.8 | 0.88 ± 0.1 | 7.36 |
| **20** | H | $CH_3$ | 5.3 ± 0.1 | 3.1 ± 0.4 | 7.50 |
| **21** | $CH_3$ | $CH_3$ | 0.169 ± 0.006 | 0.12 ± 0.0001 | - |
| **24** | H | OH | 193.9 ± 10.5 | 17.9 ± 2.6 | - |
| **25** | $CH_3$ | OH | 141.2 ± 17.9 | 9.1 ± 2.4 | - |
| **27** | H | $OCH_3$ | 132.7 ± 13.1 | 9.8 ± 0.4 | - |
| **28** | $CH_3$ | $OCH_3$ | 5 ± 0.3 | 0.55 ± 0.03 | - |
| **37** (*R*) | $CH_3$ | $CH_3$ | 0.038 ± 0.0001 | 0.0014 ± 0.00007 | 7.84 |
| **38** (*S*) | $CH_3$ | $CH_3$ | 1.91 ± 0.1 | 0.013 ± 0.001 | 8.37 |

[a] Docking scores are Surflex-Dock scores, in which higher numbers represent higher affinity. N/A: not applicable, N/D: not determined

against DHFR from both *C. hominis* and *T. gondii*. The structures of the enzymes guided the design of derivative compounds such that large increases in potency were achieved during the synthesis of just 14 compounds from the parent, TMP. While we have focused on increasing potency here, the lead-like nature of these compounds allows the incorporation of additional functionality for selectivity without overstepping molecular weight boundaries.

## Chemistry, Modeling, and Biological Evaluation

**Structural Analysis of DHFR from *C. hominis* and *T. gondii*.** We have previously reported the crystal structure of ChDHFR with different ligands;[12,13] however, there is no experimentally determined structure of TgDHFR. In previous work[11] we created a homology model of TgDHFR based on the closely related structure of DHFR from *Mus musculus* (PDB ID: 1U70[14]). The TgDHFR model was minimized, and a Ramachandran analysis showed that the backbone geometry fell outside allowed regions for only six residues in loop regions. The model was further validated by docking eleven inhibitors with determined $IC_{50}$ values into the active site and achieving a 50.2% correlation with the measured inhibition constants.

Superpositions of the crystal structure of ChDHFR and the homology model of TgDHFR show that the two enzymes are very similar, both in overall fold and in the identity and arrangement of many active site residues (Figure 2a). Surrounding the pteridine ring system of methotrexate (Figure 2b), a potent inhibitor modeled into both sites, are residues that are conserved between the two species: an aspartic acid residue (32 in Ch, 31 in Tg) forms an electrostatic interaction with the protonated N1 and a hydrogen bond with the amino group at position 2 as well as Thr (134 in Ch, 172 in Tg), Val (9 in Ch, 8 in Tg) and Phe (36 in Ch and 35 in Tg) that form van der Waals interactions. The linker between the pteridine and the *para*-aminobenzoic acid (*p*ABA) is surrounded by one conserved Thr (58 in Ch and 83 in Tg) and one nonconserved residue: Cys 113 in Ch and Val 151 in Tg. The *p*ABA ring is bound in a less well-conserved hydrophobic pocket comprised of Ile 62 in Ch (Met 87 in Tg), Leu 67 in Ch (Leu 94 in Tg) and Leu 33 in Ch (Phe 32 in Tg).

In both species, models of TMP (**2**) show electrostatic and hydrogen bond interactions between the protonated N1 and the amino group at the C2 position of the pyrimidine ring and the conserved Asp in the active site. This interaction between the 2,4-diaminopyrimidine and an acidic residue in the active site is conserved across many species of DHFR.[3,12,15−17] However, the linker region of TMP appears to be too short to extend the trimethoxyphenyl ring fully into the hydrophobic pocket normally occupied by the *p*ABA ring of MTX, possibly explaining the lower *in vitro* potency of TMP against these species. Based on these structural analyses, a relatively simple strategy emerged to increase the potency of TMP for both of the target organisms by extending the length of the linker between the two aromatic rings.

**Design and Synthesis of Extended TMP Analogues.** In order to test the hypothesis that extending the distance between the diaminopyrimidine and phenyl rings of TMP would achieve greater potency against ChDHFR and TgDHFR, we explored

**Scheme 2**[a]

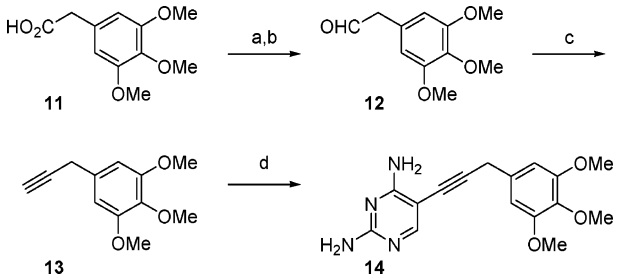


[a] Reagents and conditions: (a) LAH, $Et_2O$, 0 °C, 1 h (93%); (b) Dess−Martin periodinane, DCM, 25 °C, 1 h (96%); (c) dimethyl (1-diazo-2-oxopropyl)phosphonate, $K_2CO_3$, MeOH, 0 °C, 1 h (52%); (d) **5**, $Pd(PPh_3)_2Cl_2$, CuI, $Et_3N$, DMF, 100 °C, 2 h (80%).

the use of a two-carbon linker in place of the single methylene bridge found in TMP. In previous work, the synthesis of six 5-ethynylpyrimidine derivatives with non-benzyl moieties had been reported[18] and these compounds appeared to inhibit *T. gondii* and two species of fungal DHFR. TMP derivatives containing saturated aliphatic (**10**), *cis* (**8**) and *trans*-olefinic (**9**), or acetylenic (**7**) linkers were docked into the crystal structure of ChDHFR, chosen because it was determined from experimental data. TMP analogues with rigid olefinic and acetylenic linkers allowed the diaminopyrimidine to dock into the proper orientation but these linkers prevented the trimethoxyphenyl ring from occupying the biologically relevant hydrophobic pocket. However, the high degree of flexibility allowed by the saturated ethylene bridge appeared to allow both rings to occupy their respective pockets. A direct and high-yielding synthetic route to **10** (Scheme 1) was developed that incidentally allowed for the preparation of this entire series of TMP analogues.

The commercially available diaminopyrimidine **4** could be directly iodinated at the C5 position to give **5.** Direct conversion to the tolan derivative **7** was achieved through a palladium-catalyzed Sonagashira coupling reaction[18,19] with trimethoxyphenyl acetylene, **6**, prepared by Corey−Fuchs[20] extension of the corresponding aldehyde. Catalytic hydrogenation of **7** was next employed to prepare the fully saturated analogue **10**. Interestingly, under standard hydrogenation conditions, the second reduction was found to be quite slow, and the *cis*-olefinic linker **8** could be isolated and purified. Equilibration to the more thermodynamically stable *trans*-isomer **9** was accomplished by treatment with iodine and allowed easy access to the entire two-carbon bridge series. Examination of these extended TMP analogues in standard enzyme inhibition assays revealed that all four analogues were inactive (Table 1). Poor activity was anticipated for analogues **7**, **8**, and **9** from the docking studies, but not for the fully saturated derivative **10**.

**Design and Synthesis of the Propargyl-Linked Series.** The failure to obtain active compounds in this series (**7**−**10**) was presumed to be due to a mixture of entropic and conformational effects. While compound **10** can easily adopt a conformation that allows both aromatic rings to occupy their respective binding pockets, it does so at a significant entropic penalty induced by the organization around the highly flexible linker

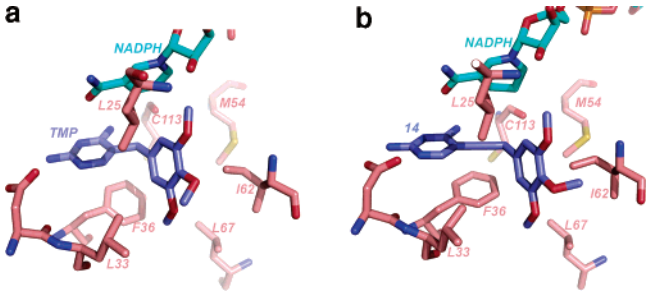


**Figure 3.** (a) TMP modeled in the active site of ChDHFR. (b) Compound **14** modeled in the active site of ChDHFR.

(increase from two rotatable bonds in TMP to three in **10**). The other three compounds in this series have lower internal entropy but cannot reach conformations that are productive for binding. Redesign in this series pointed toward analogues with a limited number of rotatable bonds but more freedom for the two aromatic rings to find appropriate binding pockets. The use of a three-carbon propargylic tether appeared as a potential design, as it maintains the same number of degrees of freedom as TMP but allows the two rings to explore more structural space independent of the other. Docking of the two alternative propargyl-linked structures revealed that attaching the trimethoxyphenyl group to the methylene carbon rather than the alkyne carbon would be preferred.

The homologated alkyne **13** required for the synthesis was prepared in three operations from the commercially available acid **11** (Scheme 2). Reduction of **11** to the alcohol, followed by Dess−Martin oxidation, produced the corresponding aldehyde that was condensed with the Ohira−Bestmann[20] reagent to directly deliver the terminal acetylene **13**. This alkyne was engaged in Sonagashira coupling reactions with the previously described **5** to give the parent compound **14**. It was found that **14** inhibited ChDHFR with an $IC_{50}$ value of 86 $\mu$M and TgDHFR with an $IC_{50}$ value of 22 $\mu$M (Table 1).

While the propargyl extended compound (**14**) did inhibit the enzyme, its activity was unexpectedly lower than that of TMP. Therefore we reexamined models of TMP and **14** in ChDHFR to better understand this discrepancy (Figure 3). Extending the phenyl ring did appear to increase interactions with the hydrophobic pocket, specifically with Ile 62 and Leu 67, as predicted. However, the extension of the phenyl also caused a loss of lipophilic interactions with Leu 25, Leu 33, and Phe 36 and created a pocket near the C6 position of the pyrimidine ring. This area is normally occupied by secondary ring fusions in potent inhibitors such as MTX. Further analysis of the docked TMP and **14** also revealed a second empty space near Cys 113 within the binding site.

A combination of Flo98[21] and Surflex-Dock[22,23] within the Sybyl environment were used to assess docking scores for methyl substitutions at the pyrimidine and propargyl locations on **14**. Flo98 performs a Monte Carlo search for the best docking poses into a flexible target and saves an ensemble of protein: ligand complexes with associated energy scores. Surflex-Dock does not dock into the binding site but rather uses a protomol[24] target that is created by probing the active site with small

**Scheme 3**

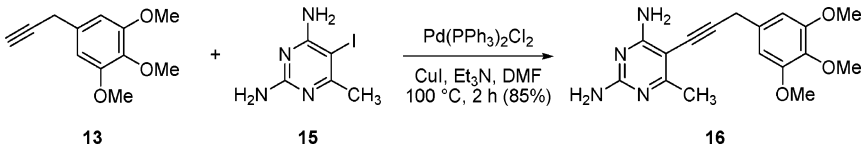

**Scheme 4**[a]

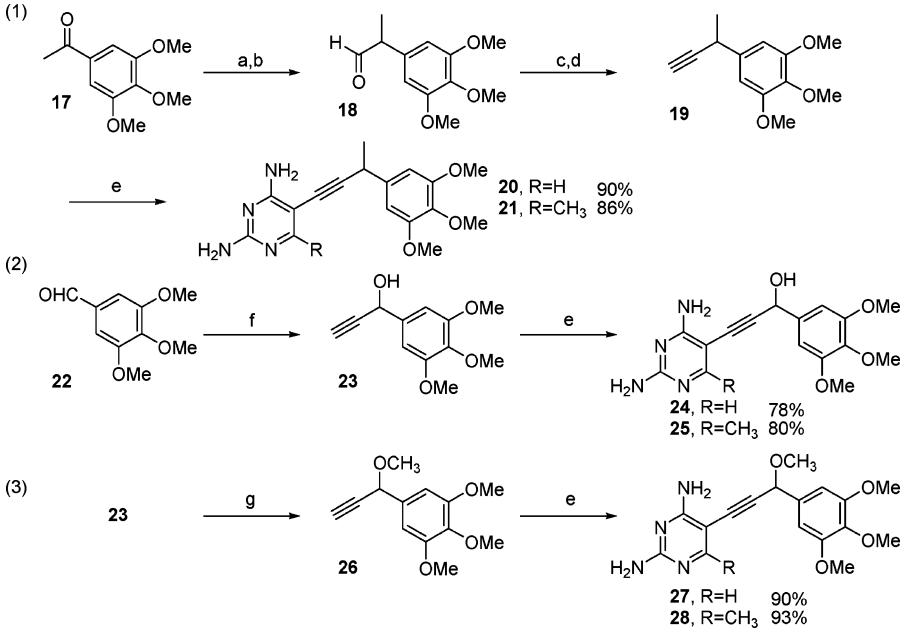


[a] Reagents and conditions: (a) $Ph_3P{=}CHOMe$, *n*-BuLi, THF, 0 °C, 1 h (73%); (b) concd HCl, THF, reflux, 3 h (93%); (c) $CBr_4$, $PPh_3$, DCM, 0 °C, 35 min (75%); (d) Mg, THF, reflux, 1.5 h (70%); (e) **5** or **15**, $Pd(PPh_3)_2Cl_2$, CuI, $Et_3N$, DMF, 100 °C, 2 h; (f) ethynylmagnesium bromide, THF, 0 °C → 25 °C, 1 h (95%); (g) NaH, $Me_2SO_4$, THF, 25 °C, 1 h (90%)

**Scheme 5**[a]

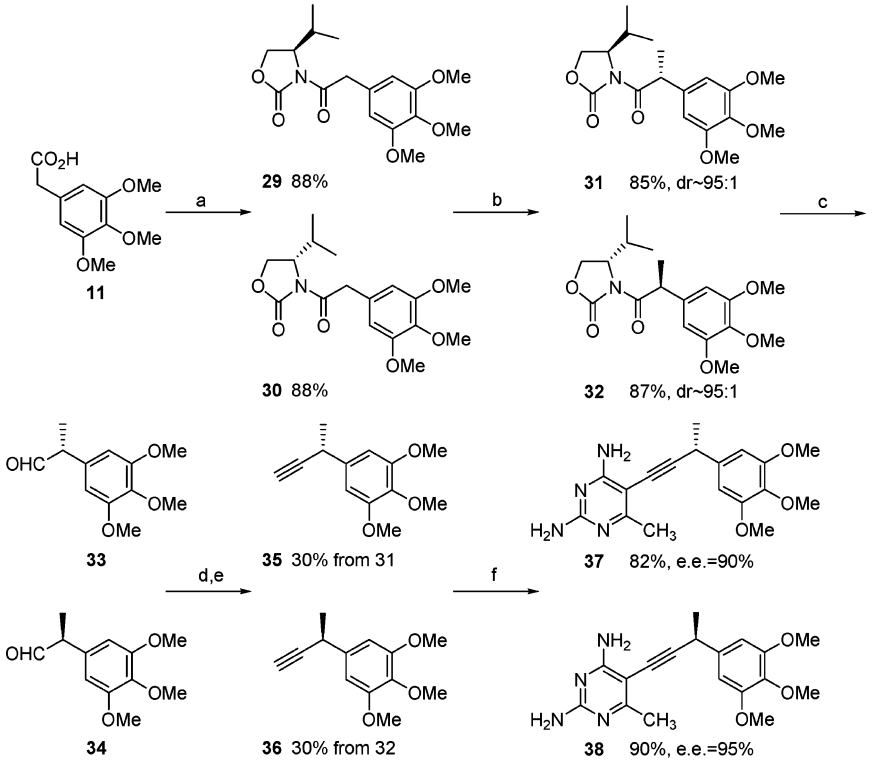


[a] Reagents and conditions: (a) pivaloyl chloride, $Et_3N$, oxazolidinone, *n*-BuLi, THF, −78 °C → 25 °C, 3 h; (b) LHMDS, MeI, THF, −78 °C → 0 °C, 2 h; (c) DIBAL-H, DCM, −78 °C, 2 h; (d) $CBr_4$, $PPh_3$, DCM, 0 °C, 35 min; (e) Mg, THF, reflux, 1 h; (f) **15**, $Pd(PPh_3)_2Cl_2$, CuI, $Et_3N$, DMF, 100 °C, 2 h.

molecular fragments. Ligands are then fragmented and built into the protomol based on an empirical scoring function[25] that accounts for hydrophobic, polar, repulsive, entropic, and solvation terms.[26]

The docking score of **14** with individual methyl groups in the two noted pockets was greater than that of the unsubstituted compound **14**, while the analogue with methyl groups in both pockets simultaneously presented the highest score (Table 1). Since Surflex-Dock cannot assess a racemic compound, both the *R* and *S* enantiomers of the compound with a methyl at the propargyl position were evaluated. Both appear equally viable upon visual analysis and had many of the same interactions with nearby residues. All complexes presented the 'correct' 2,4-diaminopyrimidine positioning within the binding site, with hydrogen bonds to Val 9, Val 10, Asp 32, and Thr 134.

The propargyl scaffold appeared to be superior to TMP for placing substituents in these pockets as well as for synthetic accessibility. The analogous substitutions on TMP have a large

impact in the conformational distribution while interactions between the C6 substitution and the aryl ring in the propargyl series were computationally shown to not be significant. It proved possible to extend the previous success of the Sonagashira coupling reactions (Scheme 3) to install substitution at C6 of the extended inhibitors.

Cross-coupling of acetylene **13** with the known[18] iodopyrimidine **15** (prepared from commercially available 2-amino-4-chloro-6-methylpyrimidine by amination and iodination) yielded the C6-methyl derivative **16**. As predicted by both visual analysis of the docked compound and the docking scores (Table 1), compound **16** displayed improved potency over the unsubstituted analogue (**14**) against both enzymes with $IC_{50}$ values of 10.2 and 0.88 $\mu$M against ChDHFR and TgDHFR, respectively (Table 1).

In previous work,[4] we explored the second vacant pocket near residue Cys 113 in ChDHFR by employing substitutions on the methylene bridge of TMP. C7-methyl TMP (*rac*) has an $IC_{50}$ value of 340 $\mu$M, and C7-ethyl TMP (*rac*) showed moderate improvement over TMP, with an $IC_{50}$ value of 4 $\mu$M. Again, modifying the propargyl extended scaffold of **14** and **16** appeared to be a better route for exploiting this pocket, as the substitution would potentially form higher affinity interactions with Cys 113. We examined a small series of three different substituents (methyl, hydroxyl, and methoxy) at the propargylic position in an attempt to increase the potency of compounds **14** and **16**. The new terminal acetylenes for these derivatives were prepared, as racemates, in a straightforward manner (Scheme 4).

The commercially available trimethoxyacetophenone **17** was homologated to the aldehyde **18** through Wittig condensation and hydrolysis of the resulting enol ether.[27] A modified Corey−Fuchs homologation[28] provided the racemic acetylene **19** that was coupled with both iodopyrimidines **5** and **15** to produce the corresponding analogues **20** and **21**. Installation of a hydroxyl or methoxy substituent could be accomplished in a straightforward manner from aldehyde **22**. This was converted to the propargyl alcohol **23** through the addition of acetylide, and then standard Sonagashira couplings on **23** gave analogues **24** and **25** in high yield. Alternatively, the alcohol could be converted to the corresponding methyl ether **26** under standard conditions and cross-coupled in an analogous manner to deliver pyrimidines **27** and **28**. Again, as predicted from the docked complexes, the methyl-substituted propargyl compound, **21**, exhibited marked improvement in potency with $IC_{50}$ values of 169 nM and 120 nM against ChDHFR and TgDHFR, respectively. The hydroxy- and methoxy-substituted propargyl compounds did not exhibit the same improvement (Table 1).

With the excellent performance of the doubly methylated derivative **21** in ChDHFR and TgDHFR inhibition assays, it was logical to examine the individual isomers at the stereogenic center to determine if one of the enantiomers was more active than the other. To accomplish the synthesis of the two enantiomeric analogues, we employed an Evans oxazolidinone-mediated asymmetric alkylation[29] (Scheme 5).

Addition of two different lithio oxazolidinones to the mixed anhydride derived from acid **11** led to imides **29** and **30** that could be alkylated to produce **31** and **32** with fairly high diastereoselectivity. Unfortunately, the minor diastereomer could not be removed during purification and was taken on in the following steps. Partial reduction of the imide with DIBAL-H produced the aldehydes **33** and **34** that were immediately homologated as described in the racemic synthesis to give terminal alkynes **35** and **36**. Cross-coupling with iodopyrimidine **15** gave the two enantiomers **37** and **38** in 90 and 95% ee, respectively as determined by HPLC analysis using a chiral stationary phase column.

**Table 2.** Ligand Efficiency of Selected Compounds

| compound | ChDHFR | TgDHFR |
|---|---|---|
| TMP | 0.32 | 0.33 |
| MTX | 0.32 | 0.33 |
| 14 | 0.24 | 0.28 |
| 16 | 0.29 | 0.35 |
| 37 | 0.41 | 0.49 |

The two enantiomers exhibited quite different affinities for the protozoal enzymes with the *R* enantiomer inhibiting ChDHFR with an $IC_{50}$ value of 38 nM and TgDHFR with an $IC_{50}$ value of 1.4 nM. The opposite enantiomer, *S*, inhibited ChDHFR and TgDHFR with $IC_{50}$ values of 1.9 $\mu$M and 13 nM, respectively.

In addition to an improvement in potency, this series of compounds shows an improvement in ligand efficiency (Table 2). The ligand efficiency of **14** decreased relative to TMP since the additional molecular weight due to the acetylene did not lead to appropriate increases in potency. However, the methyl group additions to the propargyl scaffold exhibited large increases in ligand efficiency. In the ChDHFR case, the C6 and propargyl methyl groups yielded 16% and 43% increases in ligand efficiency, respectively, and for TgDHFR, the C6 and propargyl methyl groups yielded 26% and 44% increases in ligand efficiency, respectively.

## Discussion

Through analysis of the crystal structure of ChDHFR and a validated homology model of TgDHFR, it was noted that structural features common to both enzymes may contribute to the poor activity of the archetypical inhibitor, trimethoprim. Specifically, the trimethoxyphenyl ring did not appear to extend deep enough into the hydrophobic pocket which is normally occupied by the natural substrate, dihydrofolate. Guided by this analysis, we modified the TMP structure to arrive at highly potent inhibitors (368-fold improvement for ChDHFR and 5714-fold for TgDHFR, over the parent TMP) through the synthesis of just 14 new analogues.

The models of **37** bound to ChDHFR and TgDHFR (Figure 4) nicely illustrate why this inhibitor is highly potent. In ChDHFR (Figure 4a), the C6 methyl group forms ideal van der Waals interactions with Phe 36, Leu 33, and Leu 25. The propargyl methyl group forms van der Waals interactions with Cys 113 and, remotely, with Ile 62. In TgDHFR (Figure 4b), the C6 methyl group forms van der Waals interactions with Phe 35 and Phe 32; the propargyl methyl group forms van der Waals interactions with Met 87 and Val 151.

Each enantiomer of the stereogenic propargyl position, compounds **37** and **38**, possesses higher affinity than compounds that are unsubstituted at that position (**14** or **16**). In fact, this increase in activity for each enantiomer was predicted computationally (Table 1). The fact that the *S* enantiomer was predicted to be more active than the *R*, when the biological evaluation shows that the *R* is more active, is a limitation of the computational analysis. Interestingly, in the *T. gondii* case, each enantiomer is more active in the enzyme assay than the racemic mixture (**21**). Although this appears counterintuitive, it is most likely due to the complex kinetic competition between substrate and inhibitors in the assay.

The work in this manuscript represents the first efforts in a two-tiered approach to achieving both potent and selective

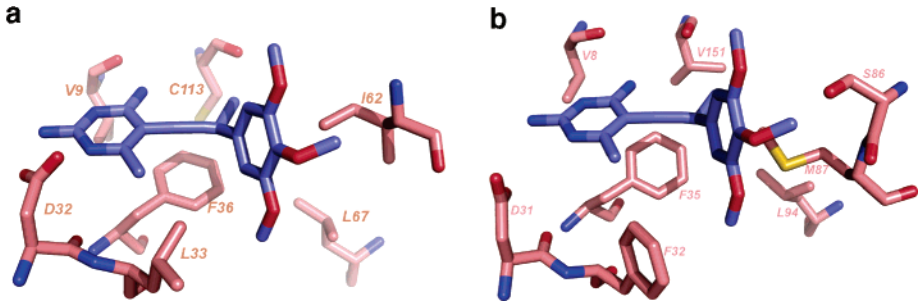


**Figure 4.** Models of **37** bound to (a) ChDHFR and (b) TgDHFR. In both cases, the inhibitor is colored blue and the protein is shown in salmon. Key residues in the active site are numbered.

inhibitors of DHFR from these parasitic protozoa. The low molecular weight of the lead compound in this work allows the installation of additional functionality to achieve selectivity against the human form of DHFR. Structural comparisons of ChDHFR and hDHFR[12] reveal that ChDHFR lacks a loop at the active site that is present in hDHFR. In future work, we plan to explore derivatives of the compounds reported here that extend functionality toward the loop, thus preventing binding to hDHFR and increasing selectivity. For TgDHFR, there are residue substitutions in the active site relative to hDHFR, including Val 5 and Met 87. Derivative compounds that exploit these differences will be used to increase selectivity.

Several heterocycles have been reported as potent inhibitors of DHFR from *T. gondii*, *Pneumocystis carinii*, and *Mycobacterium avium*. Some of these, including a 2,4-diamino-5-(2′,5′-disubstituted benzyl)pyrimidine,[30] a 2,4-diamino-6-[2′-$\omega$-carboxyalkyl)dibenzazepine]methylpteridine,[31] and three 2,4-diamino-5-deazapteridines[32,33] display nanomolar potency against TgDHFR. Like MTX, the increased potency of several of these previously reported inhibitors is related to the use of secondary ring fusions to the diaminopyrimidine core. On the basis of our analysis, these additional rings provide increased van der Waal contacts and also project functionality deeper into the hydrophobic pocket, much like the C6 substituent and the propargyl linker in our design, respectively. The acetylene moiety provides the rigidification and spacing in this system that is attributed to the second ring fusion in these other inhibitors but does so with two key additional benefits. First, there is only a slight increase in molecular weight relative to TMP, and in fact the best inhibitor presented here has an increase of only 52 Da in mass to achieve an increased potency of 368-fold for ChDHFR and 5714-fold for TgDHFR. Second, this new scaffold has much greater synthetic accessibility, owing in large part to the key Sonagashira coupling which allows for a convergent and modular approach. This type of synthetic strategy should be easily amenable to more extensive analogue development and even parallel synthetic strategies. The key features of these new TMP analogues make them excellent candidates for further development.

## Experimental Section

**Enzyme Expression, Purification, and Assays**. ChDHFR: ChDHFR−TS was expressed in *E. coli* and purified using a methotrexate agarose column (Sigma).[13] Enzyme activity assays were performed by monitoring the change in UV absorbance at 340 nm in a solution containing 50 mM tris(hydroxymethyl)methyl-2-aminoethanesulfonic acid pH 7.0, 1 mM EDTA, 75 $\mu$M 2-mercaptoethanol, 1 mg/mL bovine serum albumin, 1 mM dihydrofolate (Eprova), and 100 $\mu$M nicotinamide adenine dinucleotide phosphate (NADPH) (Sigma) and limiting concentrations of enzyme. Enzyme and inhibitor were allowed to incubate for 5 min before adding dihydrofolate to initiate the reaction. Enzyme assays were performed at least four times. $IC_{50}$ values and their standard deviations were calculated in the presence of varying concentrations of inhibitor near the $IC_{50}$ concentration.

TgDHFR: DHFR cloned from *T. gondii* DHFR−TS was determined to be insoluble after refolding at relatively low protein concentrations (>1 mg/mL). The presence of an unstructured loop region (residues 43−70) that is not present in other DHFR proteins was predicted to render the protein insoluble. These residues were removed, leaving a five residue loop region characteristic of several other species of DHFR. The removal of this unstructured loop region yielded a soluble preparation of TgDHFR at concentrations in excess of 18 mg/mL, a single species by native gel electrophoresis and with an activity level equal to *T. gondii* DHFR−TS and characteristic of other DHFR proteins after refolding. See Supporting Information for cloning and purification details. Activity assays followed the same procedure as those used for ChDHFR−TS.

**Calculation of Ligand Efficiency.** Ligand efficiency is expressed as binding energy per non-hydrogen atom ($\Delta G/N_{\text{non-hydrogen atoms}}$) where $\Delta G = -RT \ln K_d$, although $IC_{50}$ values can be substituted for $K_d$.[9] Therefore, ligand efficiencies were calculated using the quotient of $\Delta G = (1.99 \text{ cal K}^{-1} \text{ mol}^{-1})(300 \text{ K}) (\ln IC_{50})(0.001 \text{ kcal/cal})$ and the number of non-hydrogen atoms.

**Computational Modeling**. All ligands were created in Sybyl (Tripos Inc.) and checked for correct geometries. These were selectively protonated at N1 of the 2,4-diaminopyrimidine ring. Formal charges were calculated automatically.

Chain A of the 1SEJ crystal structure[12] was selected as the ChDHFR receptor. The site was prepared by removing all waters, adding hydrogens, checking for steric clashes, and calculating formal charges. The homology model of TgDHFR was created as described in the text and with further details.[11]

For docking procedures using Flo98, the active sites of both proteins were defined as all residues with an atom falling within an 11 Å sphere around the cocrystallized ligand. The automatic protomol mapping protocol within Surflex-Dock explored the entire active site and was used for docking purposes. The cocrystallized NADPH was included in the definition of the active site.

Libraries of the analogues were docked using Flo98 as discussed previously[11] and also using Surflex-Dock as a Sybyl module. All docking results were checked for correct orientation as defined by the conserved hydrogen bond interactions between the protonated N1 of the 2,4-diaminopyrimidine and Asp 32. The resulting conformational energies were also checked for steric clashes and unrealistic geometries.

**HPLC.** Samples (0.1 mg/mL in 14% $CHCl_3$, 10 mM $Na_2HPO_4$, pH 6) were analyzed isocratically (4% $CH_3CN$, 10 mM $Na_2HPO_4$ pH 6, 1.5 mL/min) using a Chrom Tech Chiral-AGP column (4.0 mm × 100 mm) and a Beckman Coulter System Gold HPLC with PDA detector.

**General.** The $^1H$ and $^{13}C$ spectra were recorded at 500 and 125 MHz, respectively, on a Varian Inova 500 spectrometer. All melting points are uncorrected. High-resolution mass spectrometry was performed on a Kratos MS-50 spectrometer by the Washington University Mass Spectrometry laboratory. Elemental analyses were provided by Atlantic Microlabs, Inc. All reagents were used directly from commercial sources unless otherwise stated.

**General Procedure for Sonagashira Couplings.** To a sealed tube was added the iodopyrimidine (1.0 mmol). DMF (5.0 mL) was added and the mixture stirred until all solids dissolved. $Pd(PPh_3)_2Cl_2$ (49.0 mg, 0.07 mmol) was added followed by CuI (13.3 mg, 0.07 mmol), $Et_3N$ (5.0 mL), and the aryl acetylene (2.0 mmol). The tube was sealed and placed into a 100 °C oil bath. The reaction was stirred at 100 °C for 2 h and cooled to room temperature. The solvent was removed and the residue purified by flash chromatography ($SiO_2$, 30 g) using 2% MeOH in $CHCl_3$ as the eluent to afford the coupled products. Analytical samples were prepared by recrystallization from MeCN.

**2,4-Diamino-5-iodopyrimidine (5).** To a flame-dried 100 mL round-bottom flask was added 2,4-diaminopyrimidine (1.0 g, 9.08 mmol) in MeOH (30 mL) followed by dropwise addition of ICl (30 mL, 29.06 mmol). The solution was stirred at 25 °C for 15 h and then the solvent removed under reduced pressure. The resulting viscous oil was stirred in $Et_2O$ (40 mL) for 45 min. The resulting solid was filtered off and washed with $Et_2O$ (3 × 10 mL) to afford the HCl salt as a yellow solid (3.14 g). The crude salt was suspended in 1.0 N NaOH (100 mL) and stirred at 25 °C for 2 h. The solids were filtered, washed with water (2 × 10 mL), and dried to afford **5** as a brown powder (1.71 g, 80%). An analytical sample was prepared by recrystallization from MeCN to give **5** as colorless crystals: $R_f$ = 0.25 (9:1, $CHCl_3$:MeOH); mp = 212−214 °C; $^1$H NMR (DMSO-$d_6$) $\delta$ 7.92 (s, 1H), 6.40 (s, 2H), 6.10 (s, 2H); $^{13}$C NMR (DMSO-$d_6$) $\delta$ 162.8, 162.7, 162.0, 61.2; HREI[$M^+$] 235.9559 (calculated $C_4H_5IN_4$: 235.9559); Anal. ($C_4H_5IN_4$) C, H, N.

**5-Ethynyl-1,2,3-trimethoxybenzene (6).** To a flame-dried 50 mL round-bottom flask was added $CBr_4$ (2.54 g, 7.65 mmol). DCM (20 mL) was added and the solution cooled to 0 °C. $Ph_3P$ (4.01 g, 15.30 mmol) was added and the solution stirred at 0 °C for 15 min. 3,4,5-Trimethoxybenzaldehyde (1.0 g, 5.10 mmol) in DCM (6.0 mL) was added dropwise. The solution was stirred at 0 °C for 5 min. The solvent was removed under reduced pressure, and the resulting oil was filtered through a plug of silica and washed with Hex:EtOAc (9:1, 500 mL; 4:1, 500 mL). The combined organics were concentrated to give the crude dibromo-olefin (2.31 g, 128%), which was dissolved in THF (60 mL) and cooled to −78 °C. n-BuLi (13.1 mL, 19.68 mmol, 1.5 M) was added dropwise and the solution stirred at −78 °C for 30 min. Saturated $NH_4Cl$ (10 mL) was added and the solution warmed to room temperature. The layers were separated, and the organics were washed with brine (10 mL), dried over anhydrous $Na_2SO_4$, and concentrated. The residue was purified by flash chromatography ($SiO_2$, 80 g) using 10% EtOAc in hexanes as the eluent to afford **6** as a colorless oil (0.770 g, 79%): $R_f$ = 0.30 (4:1, Hex:EtOAc); $^1$H NMR ($CDCl_3$) $\delta$ 6.71 (s, 2H), 3.84 (s, 3H), 3.83 (s, 6H), 3.03 (s, 1H); $^{13}$C NMR ($CDCl_3$) $\delta$ 153.1, 117.1, 109.4, 103.3, 83.8, 76.4, 61.0, 56.2, 56.1; HRFAB [M + Li] 199.0952 (calculated $C_{11}H_{12}O_3Li$: 199.0946).

**2,4-Diamino-5-(2-(3,4,5-trimethoxyphenyl)ethynyl)pyrimidine (7). 5** (236 mg) was allowed to react with **6** (384 mg) as per the general procedure to afford **7** as a white powder (270 mg, 90%): $R_f$ = 0.28 (9:1, $CHCl_3$:MeOH); mp = 202−204 °C; $^1$H NMR (DMSO-$d_6$) $\delta$ 7.94 (s, 1H), 6.90 (s, 2H), 6.37 (s, 2H), 3.79 (s, 6H), 3.67 (s, 3H); $^{13}$C NMR (DMSO-$d_6$) $\delta$ 163.4, 162.2, 159.4, 159.2, 152.8, 137.6, 118.6, 108.3, 108.2, 94.7, 89.8, 83.4, 60.2, 60.1, 56.0, 55.9; Anal. ($C_{15}H_{16}N_4O_3$) C, H, N.

**(*Z*)-2,4-Diamino-5-(3,4,5-trimethoxystyryl)pyrimidine (8). 7** (300 mg, 1.00 mmol) was placed into a 100 mL shaker flask. EtOH (30 mL) was added, and the mixture was swirled until all solids dissolved. 5% Pd/C (50 mg) was added, and the suspension was placed into a hydrogenation apparatus. The reaction was allowed to run at 45 psi $H_2$ for 5 h. The mixture was filtered through Celite and washed with EtOAc (15 mL). The solvent was removed and the residue purified by flash chromatography ($SiO_2$, 30 g) using 5% MeOH in $CHCl_3$ as the eluent to afford **8** as a white powder (100 mg, 33%, 81% borsm) which was recrystallized from MeCN: $R_f$ = 0.33 (9:1, $CHCl_3$:MeOH) ; mp = 175−177 °C; $^1$H NMR (acetone-$d_6$) $\delta$ 7.69 (s, 1H), 6.63 (s, 2H), 6.47 (d, $J$ = 11.9 Hz, 1H), 6.27 (d, $J$ = 11.9 Hz, 1H), 5.66 (s, 2H), 5.49 (s, 2H), 3.68 (s, 3H), 3.67 (s, 6H); $^{13}$C NMR ($CD_3OD$) $\delta$ 163.5, 163.3, 156.2, 154.3, 138.6, 134.0, 133.0, 122.6, 107.3, 106.4, 61.1, 56.4; HRESI [M + H] 303.1446 (calculated $C_{15}H_{19}N_4O_3$: 303.1457).

**(*E*)-2,4-Diamino-5-(3,4,5-trimethoxystyryl)pyrimidine (9). 8** (45.0 mg, 0.149 mmol) was suspended in dry THF (1.5 mL). $I_2$ (4.0 mg, 0.0149 mmol) was added and the reaction allowed to stir at 23 °C for 30 min after which time all material was in solution. The red solution was diluted with THF (5.0 mL), and saturated $Na_2S_2O_3$ (1.0 mL) was added. The layers were separated and the organics washed with water (5.0 mL) and brine (5.0 mL) and dried over anhydrous $MgSO_4$. The solvent was removed and the residue purified by flash chromatography ($SiO_2$, 5.0 g) using 5% MeOH in $CHCl_3$ as the eluent to afford **9** as a yellow powder (36 mg, 80%) which was recrystallized from MeCN: $R_f$ = 0.28 (9:1, $CHCl_3$:MeOH) ; mp = 182−184 °C; $^1$H NMR (acetone-$d_6$) $\delta$ 8.09 (s, 1H), 7.07 (d, $J$ = 15.9 Hz, 1H), 6.85 (s, 2H), 6.82 (d, $J$ = 15.9 Hz, 1H), 5.94 (s, 2H), 5.51 (s, 2H), 3.83 (s, 6H), 3.71 (s, 3H); $^{13}$C NMR ($CDCl_3$) $\delta$ 161.6, 161.3, 154.7, 153.4, 138.0, 132.9, 129.1, 119.8, 107.0, 103.4, 60.9, 56.1; HRESI [M + H] 303.1446 (calculated $C_{15}H_{19}N_4O_3$: 303.1457).

**2,4-Diamino-5-(3,4,5-trimethoxyphenethyl)pyrimidine (10). 7** (100 mg, 0.333 mmol) was placed into a 100 mL shaker flask. MeOH (20 mL) was added, and the mixture was swirled until the solids dissolved. 10% Pd/C (100 mg) was added, and the suspension was placed into a hydrogenation apparatus. The reaction was allowed to run for 10 h at 50 psi $H_2$. The solid residue was filtered through Celite and washed with methanol (10 mL). The solvent was removed, and the residue was purified by flash chromatography ($SiO_2$, 10 g) using 10% MeOH in $CHCl_3$ as the eluent to afford **10** as a white powder (88.0 mg, 87%): $R_f$ = 0.06 (9:1, $CHCl_3$:MeOH); mp = 155−157 °C; $^1$H NMR (DMSO-$d_6$) $\delta$ 7.46 (s, 1H), 6.56 (s, 2H), 6.22 (s, 2H), 5.65 (s, 2H), 3.74 (s, 6H), 3.61 (s, 3H), 2.65−2.62 (m, 2H), 2.52−2.49 (m, 2H); $^{13}$C NMR (DMSO-$d_6$) $\delta$ 162.3, 162.0, 155.0, 152.6, 137.5, 135.5, 105.8, 105.8, 60.0, 55.6, 35.0, 29.1; Anal. ($C_{15}H_{20}N_4O_3$) C, H, N.

**1,2,3-Trimethoxy-5-(prop-2-ynyl)benzene (13).** To a flame-dried 1 L flask was added $LiAlH_4$ (3.85 g, 101.4 mmol). $Et_2O$ (250 mL) was added and the suspension cooled to 0 °C. Trimethoxyphenylacetic acid (15.3 g, 67.6 mmol) in $Et_2O$ (50 mL) was added dropwise and the reaction allowed to stir at 0 °C for 1 h. Water (50 mL) was added and the solution warmed to room temperature. The solids were filtered off and washed with $Et_2O$ (3 × 25 mL). The combined organics were washed with brine (25 mL), dried over anhydrous $Na_2SO_4$, and concentrated to give the crude alcohol (13.4 g, 93%). The crude alcohol (13.3 g, 62.7 mmol) was dissolved in DCM (125 mL). Dess−Martin periodinane (39.8 g, 94.0 mmol) was added and the reaction stirred at room temperature for 1 h. Saturated $NaHCO_3$:saturated $Na_2S_2O_3$ (1:1, v:v, 20 mL) was added and the reaction stirred for 30 min. The organic layer was washed with brine (25 mL), dried over anhydrous $Na_2SO_4$, and concentrated to give aldehyde **12** (13.1 g, 96%). Spectra were identical to literature values.[34]

The Ohira−Bestmann reagent (15.1 g, 78.6 mmol) was dissolved in MeOH (260 mL) and the reaction cooled to 0 °C. **12** (11.0 g, 52.3 mmol) was added followed by $K_2CO_3$ (15.9 g, 115.0 mmol). The reaction was allowed to stir at 0 °C for 1 h and warmed to room temperature, and the solids were filtered. The organics were concentrated and the residue purified by flash chromatography ($SiO_2$, 500 g) using 10% EtOAc in hexanes as the eluent to afford **13** as a colorless oil (5.61 g, 52%): $R_f$ = 0.20 (10%EtOAc); $^1$H NMR ($CDCl_3$) $\delta$ 6.58 (s, 2 H), 3.86 (s, 6 H), 3.83 (s, 3H), 3.55 (s, 2 H), 2.22 (s, 1 H); $^{13}$C ($CDCl_3$) $\delta$ 153.28, 136.75, 131.70, 104.89, 81.87, 70.69, 60.80, 56.06, 24.99; HREI[$M^+$] 206.0943 (calculated $C_{12}H_{14}O_3$: 206.0943).

**2,4-Diamino-5-(3-(3,4,5-trimethoxyphenyl)prop-1-ynyl)pyrimidine (14). 5** (236 mg) was allowed to react with **13** (412 mg) as per the general procedure to afford **14** as a white powder (251 mg, 80%): $R_f$ = 0.23 (9:1, $CHCl_3$:MeOH); mp = decomposed above 190 °C; $^1$H NMR (DMSO-$d_6$) $\delta$ 7.84 (s, 1H), 6.71 (s, 2H), 6.26 (s, 2H), 3.80 (s, 2H), 3.77 (s, 6H), 3.63 (s, 3H); $^{13}$C NMR (DMSO-$d_6$) $\delta$ 163.8, 162.2, 158.7 152.8, 136.0, 132.8, 105.2, 93.1, 90.1 76.5, 60.1, 55.8, 25.6; Anal. ($C_{16}H_{18}N_4O_3$) C, H, N.

**2,4-Diamino-5-iodo-6-methylpyrimidine (15).** To a 100 mL steel pressure vessel was added 2-amino-4-chloro-6-methylpyrimidine (4.00 g, 28.00 mmol). A saturated solution of $NH_3$ in MeOH (40 mL) was added and the vessel sealed. The pressure vessel was placed into a 160 °C oil bath and heated for 15 h. The vessel was cooled to 0 °C and opened and the solvent removed to give the crude diaminopyrimidine (4.4 g) as the HCl salt. The crude salt was dissolved in MeOH (82.5 mL), and ICl (82.5 mL) was added dropwise over 50 min. The reaction was stirred at 25 °C for 14 h and the solvent removed. The viscous oil was stirred in $Et_2O$ (300 mL) for 30 min. The resulting solid was filtered and washed with $Et_2O$ (3 × 20 mL) to give the crude iodinated pyrimidine as a yellow solid (10.1 g). The solids were suspended in 1.0 N NaOH (300 mL) and stirred at 25 °C for 2 h. The solids were filtered, washed with water (2 × 20 mL), and allowed to dry to afford **15** as a white powder (5.6 g, 80%). An analytical sample was prepared by recrystallization from MeCN to give **15** as colorless crystals: $R_f$ = 0.25 (9:1, $CHCl_3$:MeOH); mp = 154−156 °C; $^1$H NMR (DMSO-$d_6$) $\delta$ 6.38 (s, 2H), 6.09 (s, 2H), 2.24 (s, 3H); $^{13}$C NMR (DMSO-$d_6$) $\delta$ 166.7, 163.0, 162.3, 63.8, 28.4; HREI[$M^+$] 249.9715 (calculated $C_5H_7IN_4$: 249.9715); Anal. ($C_5H_7IN_4$) C, H, N.

**2,4-Diamino-5-(3-(3,4,5-trimethoxyphenyl)prop-1-ynyl)-6-methylpyrimidine (16). 15** (250 mg) was allowed to react with **13** (412 mg) as per the general procedure to afford **16** as a white powder (280 mg, 85%): $R_f$ = 0.31 (9:1, $CHCl_3$:MeOH); mp = 164−166 °C; $^1$H NMR (DMSO-$d_6$) $\delta$ 6.72 (s, 2H), 6.42 (s, 2H), 3.85 (s, 2H), 3.76 (s, 6H), 3.63 (s, 3H), 2.24 (s, 3H); $^{13}$C NMR (DMSO-$d_6$) $\delta$ 165.0, 164.3, 159.7, 152.8, 135.9, 132.8, 105.0, 96.3, 89.3, 75.8, 60.0, 55.8, 25.7, 21.7; HRFAB [M + Li] 335.1679 (calculated $C_{17}H_{20}N_4O_3Li$: 335.1695).

**5-(But-3-yn-2-yl)-1,2,3-trimethoxybenzene (19).** To a flame-dried 250 mL round-bottom flask was added methoxymethyltriphenylphosphonium bromide (10.28 g, 30.0 mmol). THF (100 mL) was added and the solution cooled to 0 °C. n-BuLi (14.0 mL, 30.0 mmol, 2.2 M) was added dropwise and the solution stirred at 0 °C for 30 min. 3,4,5-Trimethoxyacetophenone (5.26 g, 25.0 mmol) in THF (25 mL) was added dropwise. The reaction was stirred at 0 °C for 30 min, and then water (30 mL) was added. The layers were separated, and the aqueous layer was extracted with $Et_2O$ (3 × 20 mL). The combined organics were washed with brine (30 mL), dried over anhydrous $Na_2SO_4$, and concentrated. The residue was purified by flash chromatography ($SiO_2$, 50 g) using 5% EtOAc in hexanes as eluent to afford the enol ether (4.35 g, 73%).

The enol ether (4.35 g, 18.26 mmol) was dissolved in THF (37.0 mL). Concentrated HCl (3.0 mL) was added and the solution heated to reflux. The solution was stirred at reflux for 3 h and allowed to cool to room temperature. Water (10 mL) was added, and the organics were washed with sat. $NaHCO_3$ (10 mL) and brine (10 mL), dried over anhydrous $Na_2SO_4$, and concentrated. The residue was purified by flash chromatography ($SiO_2$, 50 g) using 20% EtOAc in hexanes as the eluent to afford **18** (3.82 g, 93%). Spectra were the identical to literature values.[27]

$CBr_4$ (8.47 g, 25.55 mmol) was dissolved in DCM (150 mL) and cooled to 0 °C. $Ph_3P$ (13.4 g, 51.09 mmol) was added and the solution stirred at 0 °C for 5 min. **18** (3.82 g, 17.03 mmol) in DCM (20 mL) was added dropwise. The reaction was stirred at 0 °C for 30 min and then poured into ice-cooled $Et_2O$ (500 mL). The solids were filtered through Celite and washed with $Et_2O$ (3 × 50 mL). The combined organics were concentrated. The residue was filtered through a plug of silica and washed with hexanes (100 mL) followed by 10% EtOAc in hexanes (5 × 100 mL). The combined organics were concentrated to give the intermediate dibromide (4.86 g, 75%) which was used directly for the next reaction.

Mg (0.621 g, 25.57 mmol) was suspended in THF (2.0 mL). 1,2-Dibromoethane (0.442 mL, 5.12 mmol) was added and the reaction stirred at 25 °C for 30 min. The dibromide (4.86 g, 12.79 mmol) in THF (11.0 mL) was added dropwise and the solution heated to reflux where it was stirred for 1 h. The solution was cooled to room temperature and the solvent removed. The residue was purified by flash chromatography ($SiO_2$, 150 g) using 10% EtOAc in hexanes as the eluent to afford **19** as a colorless oil (1.97 g, 70%): $R_f$ = 0.29 (4:1, Hex:EtOAc); $^1$H NMR ($CDCl_3$) $\delta$ 6.62 (s, 2H), 3.88 (s, 6H), 3.84 (s, 3H), 3.74−3.69 (m, 1H), 2.29 (d, $J$ = 2.7 Hz, 1H), 1.52 (d, $J$ = 7.1 Hz, 3H); $^{13}$C NMR ($CDCl_3$) $\delta$ 153.4, 138.5, 136.9, 104.0, 104.0, 87.2, 70.5, 61.0, 56.3, 32.1, 24.5; HRFAB [M + Li] 227.1243 (calculated $C_{13}H_{16}O_3Li$: 227.1259).

**2,4-Diamino-5-(3-(3,4,5-trimethoxyphenyl)but-1-ynyl)pyrimidine (20). 5** (236 mg) was allowed to react with **19** (440 mg) as per the general procedure to afford **20** as a yellow powder (295 mg, 90%): $R_f$ = 0.29 (9:1, $CHCl_3$:MeOH); mp = 220−222 °C; $^1$H NMR (DMSO-$d_6$) $\delta$ 7.85 (s, 1H), 6.75 (s, 2H), 6.28 (s, 2H), 3.99 (q, $J$ = 6.8 Hz, 1H), 3.78 (s, 6H), 3.63 (s, 3H), 1.50 (d, $J$ = 7.1 Hz, 3H); $^{13}$C NMR (DMSO-$d_6$) $\delta$ 163.7, 152.8, 139.3, 136.0, 104.2, 104.1, 97.9, 76.2, 60.0, 60.0, 55.9, 55.8, 32.3, 24.3; Anal. ($C_{17}H_{20}N_4O_3$) C, H, N.

**2,4-Diamino-5-(3-(3,4,5-trimethoxyphenyl)but-1-ynyl)-6-methylpyrimidine (21). 15** (250 mg) was allowed to react with **19** (440 mg) as per the general procedure to afford **21** as a white powder (294 mg, 86%): $R_f$ = 0.29 (9:1, $CHCl_3$:MeOH); mp = 191−193 °C; $^1$H NMR (DMSO-$d_6$) $\delta$ 6.76 (s, 2H), 6.19 (s, 2H), 4.02 (q, $J$ = 7.1 Hz, 1H), 3.77 (s, 6H), 3.63 (s, 3H), 2.21 (s, 3H), 1.51 (d, $J$ = 7.1 Hz, 3H); $^{13}$C NMR (DMSO-$d_6$) $\delta$ 167.0, 164.1, 161.0, 152.8, 139.4, 136.0, 104.0, 100.8, 88.6, 76.4, 60.0, 55.8, 32.5, 24.6, 22.5; Anal. ($C_{18}H_{22}N_4O_3$) C, H, N.

**1-(3,4,5-Trimethoxyphenyl)prop-2-yn-1-ol (23).** To a flame-dried 250 mL round-bottom flask was added 3,4,5-trimethoxybenzaldehyde (3.92 g, 20.0 mmol). THF (40 mL) was added and the solution was cooled to 0 °C. Ethynylmagnesium bromide (48.0 mL, 24.0 mmol, 0.5 M) was added dropwise. The solution was stirred at 0 °C for 30 min, warmed to 25 °C, and stirred for 30 min. Saturated $NH_4Cl$ (5.0 mL) was added, and the layers were separated. The aqueous layer was extracted with $Et_2O$ (3 × 5 mL). The combined organics were washed with brine (10 mL), dried over anhydrous $Na_2SO_4$, and concentrated. The residue was purified by flash chromatography ($SiO_2$, 100 g) using 20% EtOAc in hexanes as the eluent to afford **23** as a yellow oil (4.22 g, 95%): $R_f$ = 0.25 (1:1, Hex:EtOAc); $^1$H NMR ($CDCl_3$) $\delta$ 6.77 (s, 2H), 5.39 (dd, $J$ = 5.5, 2.0 Hz, 1H), 3.86 (s, 6H), 3.82 (s, 3H), 2.76 (d, $J$ = 5.9 Hz, 1H); $^{13}$C NMR ($CDCl_3$) $\delta$ 153.4, 138.1, 135.9, 103.7, 83.6, 74.9, 64.5, 61.0, 56.2; HRFAB [M + Li] 229.1054 (calculated $C_{12}H_{14}O_4$-Li: 229.1052).

**3-(2,4-Diaminopyrimidin-5-yl)-1-(3,4,5-trimethoxyphenyl)-prop-2-yn-1-ol (24). 5** (236 mg) was allowed to react with **23** (444 mg) as per the general procedure to afford **24** as a yellow powder (257 mg, 78%): $R_f$ = 0.12 (9:1, $CHCl_3$:MeOH); mp = 203−205 °C; $^1$H NMR (DMSO-$d_6$) $\delta$ 7.84 (s, 1H), 6.83 (s, 2H), 6.34 (s, 2H), 6.01 (d, $J$ = 5.6 Hz, 1H), 5.50 (d, $J$ = 5.4 Hz, 1H), 3.78 (s, 6H), 3.65 (s, 3H); $^{13}$C NMR (DMSO-$d_6$) $\delta$ 163.8, 162.3, 158.2, 152.7, 138.3, 136.7, 109.3, 103.6, 96.3, 79.3, 63.4, 60.0, 55.8; Anal. ($C_{16}H_{18}N_4O_4$) C, H, N.

**3-(2,4-Diamino-6-methylpyrimidin-5-yl)-1-(3,4,5-trimethoxyphenyl)prop-2-yn-1-ol (25). 15** (250 mg) was allowed to react with **23** (444 mg) as per the general procedure to afford **25** as a yellow powder (275 mg, 80%): $R_f$ = 0.12 (9:1, $CHCl_3$:MeOH); mp = 174−176 °C; $^1$H NMR (DMSO-$d_6$) $\delta$ 6.85 (s, 2H), 6.27 (s, 2H), 5.98 (d, $J$ = 5.6 Hz, 1H), 5.53 (d, $J$ = 5.4 Hz, 1H), 3.78 (s, 6H), 3.65 (s, 3H), 2.19 (s, 3H), 1.51 (d, $J$ = 7.1 Hz, 3H); $^{13}$C NMR (DMSO-$d_6$) $\delta$ 167.1, 164.3, 161.2, 152.7, 138.3, 136.7, 103.7, 99.1, 87.9, 79.5, 63.6, 60.0, 55.8, 22.5; HRFAB [M + Li] 351.1638 (calculated $C_{17}H_{20}N_4O_4Li$: 351.1645).

**1,2,3-Trimethoxy-5-(1-methoxyprop-2-ynyl)benzene (26).** To a flame-dried 100 mL round-bottom flask was added NaH (0.240 mg, 6.0 mmol) that had been prewashed with pentane (3 × 15 mL) and dried. THF (48 mL) was added and the suspension cooled to 0 °C. **23** (1.11 g, 5.0 mmol) in THF (2.0 mL) was added dropwise and the reaction stirred at 0 °C for 25 min. $Me_2SO_4$ (0.571 mL, 6.0 mmol) was added and the reaction stirred at 0 °C for 20 min. Water (10 mL) was added, and the layers were separated. The aqueous layer was extracted with $Et_2O$ (20 mL). The combined organics were washed with brine (20 mL), dried over anhydrous $Na_2SO_4$, and concentrated. The residue was purified by flash chromatography ($SiO_2$, 20 g) using 10% EtOAc in hexanes as the

eluent to afford **26** as a colorless oil (1.06 g, 90%): $R_f = 0.18$ (4:1, Hex:EtOAc); $^1$H NMR ($CDCl_3$) $\delta$ 6.75 (s, 2H), 5.01 (d, $J =$ 2.2 Hz, 1H), 3.88 (s, 6H), 3.84 (s, 3H), 3.45 (s, 3H), 2.68 (d, $J =$ 2.2 Hz, 1H); $^{13}$C NMR ($CDCl_3$) $\delta$ 153.4, 138.2, 133.7, 104.4, 81.3, 76.0, 73.1, 61.0, 56.3, 56.2; HRFAB [M + Li] 243.1208 (calculated $C_{13}H_{16}O_4Li$: 243.1209).

**2,4-Diamino-5-(3-methoxy-3-(3,4,5-trimethoxyphenyl)prop-1-ynyl)pyrimidine (27). 5** (236 mg) was allowed to react with **26** (473 mg) as per the general procedure to afford **27** as an orange powder (310 mg, 90%): $R_f = 0.31$ (9:1, $CHCl_3$:MeOH); mp = 184−186 °C; $^1$H NMR (DMSO-$d_6$) $\delta$ 7.91 (s, 1H), 6.82 (s, 2H), 6.40 (s, 2H), 5.30 (s, 1H), 3.79 (s, 6H), 3.66 (s, 3H), 3.35 (s, 3H); $^{13}$C NMR (DMSO-$d_6$) $\delta$ 163.8, 162.3, 159.7, 152.8, 137.2, 134.8, 104.6, 92.6, 89.1, 81.9, 73.0, 60.0, 55.9, 55.4; Anal. ($C_{17}H_{20}N_4O_4$) C, H, N.

**2,4-Diamino-5-(3-methoxy-3-(3,4,5-trimethoxyphenyl)prop-1-ynyl)-6-methylpyrimidine (28). 15** (250 mg) was allowed to react with **26** (473 mg) as per the general procedure to afford **28** as a yellow powder (335 mg, 93%): $R_f = 0.29$ (9:1, $CHCl_3$:MeOH); mp = 127−129 °C; $^1$H NMR (DMSO-$d_6$) $\delta$ 6.84 (s, 2H), 6.37 (s, 2H), 5.34 (s, 1H), 3.78 (s, 6H), 3.66 (s, 3H), 3.35 (s, 3H), 2.23 (s, 3H); $^{13}$C NMR (DMSO-$d_6$) $\delta$ 167.6, 164.3, 161.1, 152.8, 137.2, 134.8, 104.6, 95.7, 87.5, 81.8, 73.1, 60.0, 55.8, 55.3, 22.4; HRFAB [M + Li] 359.1701 (calculated $C_{18}H_{22}N_4O_4Li$: 359.1719).

**(*R*)-4-Isopropyl-3-(2-(3,4,5-trimethoxyphenyl)acetyl)oxazolidin-2-one (29).** To a flame-dried 100 mL round-bottom flask was added 3,4,5-trimethoxyphenylacetic acid (2.10 g, 9.29 mmol). THF (25 mL) was added followed by $Et_3N$ (1.42 mL, 10.22 mmol). The solution was cooled to −78 °C. Pivaloyl chloride (1.26 mL, 10.22 mmol) was added dropwise and the solution warmed to 0 °C and stirred for 1 h. In a separate flame-dried 50 mL round-bottom flask was added (*R*)-4- isopropyloxazolidin-2-one (1.0 g). THF (20 mL) was added and the solution cooled to −78 °C. n-BuLi (6.83 mL, 9.29 mmol, 1.36 M) was added dropwise and the solution stirred at −78 °C for 15 min and then warmed to 25 °C where it was stirred for 15 min. The organolithium solution was transferred to the solution of the mixed anhydride via cannula at −78 °C. The reaction was stirred at −78 °C for 15 min, warmed to 0 °C, and stirred for 1 h. Water (10 mL) was added and the aqueous layer extracted with EtOAc (2 × 10 mL). The combined organics were washed with brine (10 mL), dried over anhydrous $MgSO_4$, and concentrated under reduced pressure. The residue was purified by flash chromatography ($SiO_2$, 30 g) using 25% EtOAc in hexanes as the eluent to afford **29** as a colorless oil (2.30 g, 88%): $R_f =$ 0.28 (1:1, Hex:EtOAc); $^1$H NMR ($CDCl_3$) $\delta$ 6.55 (s, 2H), 4.44−4.41 (m, 1H), 4.29−4.24 (m, 2H), 4.19 (dd, $J = 9.0$, 3.0 Hz, 1H), 4.12−4.07 (m, 1H), 3.82 (s, 6H), 3.80 (s, 3H), 2.36−2.30 (m, 1H), 0.87 (d, $J = 6.8$ Hz, 3H), 0.78 (d, $J = 7.1$ Hz, 3H); $^{13}$C NMR ($CDCl_3$) $\delta$ 171.2, 154.1, 153.2, 129.4, 106.7, 63.4, 60.9, 58.6, 56.2, 41.6, 28.4, 18.0, 14.7, 14.3; HRFAB [M + Li] 344.1686 (calculated $C_{17}H_{23}NO_6Li$: 344.1686).

**(*S*)-4-Isopropyl-3-(2-(3,4,5-trimethoxyphenyl)acetyl)oxazolidin-2-one (30). 30** was synthesized in an analogous manner as **29** using (*S*)-4-isopropyloxazolidin-2-one. The residue was purified by flash chromatography ($SiO_2$, 30 g) using 25% EtOAc in hexanes as the eluent to afford **30** as a colorless oil (2.30 g, 88%): $R_f = 0.28$ (1:1, Hex:EtOAc); $^1$H NMR ($CDCl_3$) $\delta$ 6.54 (s, 2H), 4.44−4.41 (m, 1H), 4.29−4.24 (m, 2H), 4.19 (dd, $J = 9.0$, 3.0 Hz, 1H), 4.12−4.07 (m, 1H), 3.82 (s, 6H), 3.80 (s, 3H), 2.36−2.30 (m, 1H), 0.87 (d, $J = 6.8$ Hz, 3H), 0.78 (d, $J = 7.1$ Hz, 3H); $^{13}$C NMR ($CDCl_3$) $\delta$ 171.2, 154.1, 153.2, 129.4, 106.7, 63.4, 60.9, 58.6, 56.2, 41.6, 28.4, 18.0, 14.6, 14.3; HRFAB [M + Li] 344.1700 (calculated $C_{17}H_{23}NO_6Li$: 344.1686).

**(*R*)-3-((*R*)-2-(3,4,5-trimethoxyphenyl)propanoyl)-4-isopropyloxazolidin-2-o ne (31).** To a flame-dried 200 mL round-bottom flask was added **29** (2.77 g, 8.21 mmol). THF (85 mL) was added and the solution cooled to −78 °C. LHMDS (12.5 mL, 12.32 mmol, 1.0 M) was added dropwise, and the reaction was allowed to stir at −78 °C for 1 h. MeI (1.54 mL, 24.63 mmol) was added and the solution stirred at −78 °C for 1 h. The solution was then warmed to 0 °C for 1 h and quenched with sat. $NH_4Cl$ (10 mL). The aqueous layer was extracted with EtOAc (2 × 10 mL). The combined organics were washed with brine (10 mL), dried over anhydrous $Na_2SO_4$, and concentrated. The residue was purified by flash chromatography ($SiO_2$, 25 g) using 25% EtOAc in hexanes as the eluent to afford **31** as a colorless oil (2.44 g, 85%, 95:1 d.r): $R_f =$ 0.37 (1:1, Hex:EtOAc); $^1$H NMR ($CDCl_3$) $\delta$ 6.56 (s, 2H), 5.07 (q, $J = 7.1$ Hz, 1H), 4.14−4.13 (m, 2H), 3.81 (s, 6H), 3.77 (s, 3H), 2.42−2.36 (m, 1H), 2.12 (s, 1H), 1.47 (d, $J = 7.1$ Hz, 3H), 0.88 (t, $J = 7.1$ Hz, 6H); $^{13}$C NMR ($CDCl_3$) $\delta$ 174.6, 153.1, 135.8, 105.2, 63.1, 60.8, 59.1, 56.1, 42.8, 28.6, 19.7, 18.0, 14.7; HRFAB [M + Li] 358.1852 (calculated $C_{18}H_{25}NO_6Li$: 358.1842).

**(*S*)-3-((*S*)-2-(3,4,5-Trimethoxyphenyl)propanoyl)-4-isopropyloxazolidin-2-o ne (32). 32** was prepared in an analogous manner as **31**. The residue was purified by flash chromatography ($SiO_2$, 25 g) using 25% EtOAc in hexanes as the eluent to afford **32** as a colorless oil (2.08 g, 87%, 95:1 d.r): $R_f = 0.37$ (1:1, Hex:EtOAc); $^1$H NMR ($CDCl_3$) $\delta$ 6.58 (s, 2H), 5.09 (q, $J = 7.1$ Hz, 1H), 4.17−4.15 (m, 2H), 3.83 (s, 6H), 3.80 (s, 3H), 2.45−2.39 (m, 1H), 2.15 (s, 1H), 1.49 (d, $J = 7.1$ Hz, 3H), 0.90 (t, $J = 7.1$ Hz, 6H); $^{13}$C NMR ($CDCl_3$) $\delta$ 174.7, 153.2, 135.9, 105.3, 63.2, 60.9, 59.2, 56.2, 42.9, 28.6, 19.8, 18.1, 14.8; HRFAB [M + Li] 358.1856 (calculated $C_{18}H_{25}NO_6Li$: 358.1842).

**General Procedure for the Synthesis of 35 and 36**. To a flame-dried 200 mL round-bottom flask was added the desired oxazolidinone (1.0 equiv). DCM (0.1 M) was added, and the solution was cooled to −78 °C. DIBAL-H (2.0 equiv) was added dropwise, and the reaction was allowed to stir at −78 °C for 2 h. Saturated $NH_4$-Cl (20 mL) was added and the solution warmed to room temperature. The solids were filtered off and washed with DCM (3 × 5 mL). The aqueous layer was extracted with EtOAc (3 × 10 mL). The combined organics were washed with brine (10 mL), dried over anhydrous $Na_2SO_4$, and concentrated. An NMR measurement of the crude material was taken, and the spectrum matched that for the racemic aldehyde **18**. The crude material was used without further purification.

$CBr_4$ (1.5 equiv) was dissolved in DCM (0.1 M) and cooled to 0 °C. $Ph_3P$ (3.0 equiv) was added and the solution stirred at 0 °C for 5 min. The crude aldehyde (1.0 equiv) in DCM (5.0 mL) was added dropwise. The reaction was allowed to stir at 0 °C for 30 min and then poured into ice-cooled $Et_2O$ (200 mL). The reaction was filtered through silica gel and washed with hexanes (100 mL) followed by 25% EtOAc in hexanes (300 mL). The organics were combined and concentrated under reduced pressure. The crude material was taken on to the next step without further purification.

Mg (2.0 equiv) was suspended in THF (1.0 mL). Dibromoethane (0.4 equiv) was added, and the suspension was stirred at 25 °C for 30 min. The crude dibromide (1.0 equiv) in THF (6.0 mL) was added dropwise, and the reaction was heated at reflux for 30 min. The solution was cooled to room temperature and the solvent removed. The residue was purified by flash chromatography to afford the respective enantioenriched acetylenes. NMR spectra were taken, and the spectra matched that for the racemic acetylene **19**.

**2,4-Diamino-5-((*R*)-3-(3,4,5-trimethoxyphenyl)but-1-ynyl)-6-methylpyrimidine (37). 31** (2.44 g, 6.94 mmol) was subjected to the general procedure to afford **35** (460 mg, 30%). 1**5** (250 mg) was allowed to react with **35** (290 mg) as per the general Sonagashira coupling procedure to afford **37** as a brown powder (280 mg, 82%, 90% ee): $R_f = 0.29$ (9:1, $CHCl_3$:MeOH); $^1$H NMR (DMSO-$d_6$) $\delta$ 6.76 (s, 2H), 6.19 (s, 2H), 4.02 (q, $J = 7.1$ Hz, 1H), 3.77 (s, 6H), 3.63 (s, 3H), 2.21 (s, 3H), 1.51 (d, $J = 7.1$ Hz, 3H); $^{13}$C NMR (DMSO-$d_6$) $\delta$ 166.9, 164.1, 160.9, 152.8, 139.4, 135.9, 104.0, 100.7, 88.6, 76.4, 60.0, 55.8, 32.5, 24.7, 22.5; HRFAB [M + Li] 349.1851 (calculated $C_{18}H_{22}N_4O_3Li$: 349.1851).

**2,4-Diamino-5-((*S*)-3-(3,4,5-trimethoxyphenyl)but-1-ynyl)-6-methylpyrimidine (38). 32** (1.66 g, 4.72 mmol) was subjected to the general procedure to afford **36** (312 mg, 30%). 1**5** (250 mg) was allowed to react with **36** (290 mg) as per the general Sonagashira coupling procedure to afford **38** as a yellow powder (308 mg, 90%, 95% ee): $R_f = 0.29$ (9:1, $CHCl_3$:MeOH); $^1$H NMR (DMSO-$d_6$) $\delta$ 6.76 (s, 2H), 6.19 (s, 2H), 4.02 (q, $J = 7.1$ Hz, 1H), 3.77 (s, 6H), 3.63 (s, 3H), 2.21 (s, 3H), 1.51 (d, $J = 7.1$ Hz, 3H);

$^{13}$C NMR (DMSO-$d_6$) $\delta$ 167.0, 164.1, 161.0, 152.8, 139.4, 136.0, 104.0, 100.8, 88.6, 76.4, 60.0, 55.8, 32.5, 24.6, 22.5; HRFAB [M + Li] 349.1851 (calculated $C_{18}H_{22}N_4O_3Li$: 349.1851).

**Acknowledgment.** The authors acknowledge Dr. Robin Couch for assistance with chiral chromatography and support of the NIH (GM067542 to A.C.A.) and NSF (#013468 to A.C.A.) for this work.

**Supporting Information Available:** Details of the preparation of TgDHFR as well as spectra for each compound. This material is available free of charge via the Internet at http://pubs.acs.org.

## References

(1) Anderson, A. Targeting DHFR in parasitic protozoa. *Drug Discovery Today* **2005**, *10*, 121−128.
(2) Chio, L.-C.; Queener, S. Identification of Highly Potent and Selective Inhibitors of Toxoplasma gondii Dihydrofolate Reductase. *Antimicrob. Agents Chemother.* **1993**, *37*, 1914−1923.
(3) Yuvaniyama, J.; Chitnumsub, P.; Kamchonwongpaisan, S.; Vanichtanankul, J.; Sirawaraporn, W.; Taylor, P.; Walkinshaw, M.; Yuthavong, Y. Insights into antifolate resistance from malarial DHFR-TS structures. *Nat. Struct. Biol.* **2003**, *10*, 357−365.
(4) Popov, V.; Chan, D.; Fillingham, Y.; Yee, W. A.; Wright, D.; Anderson, A. Analysis of complexes of inhibitors with Cryptosporidium hominis DHFR leads to a new trimethoprim derivative. *Bioorg. Med. Chem. Lett.* **2006**, *16*, 4366−4370.
(5) Rosowsky, A.; Forsch, R.; Queener, S. Inhibition of Pneumocystis carinii Toxoplasma gondii and Mycobacterium avium Dihydrofolate Reductases by 2,4-Diamino-5-[2-methoxy-5-(ω-carboxyalkoxy)benzyl]pyramidines: Marked Improvement in Potency Relative to Trimethoprim and Species Selectivity Relative to Piritrexim. *J. Med. Chem.* **2002**, *45*, 233−241.
(6) Trujillo, M.; Donald, R.; Roos, D.; Greene, P.; Santi, D. Heterologous Expression and Characterization of Bifunctional Dihydrofolate Reductase-Thymidylate Synthase Enzyme of Toxoplasma gondii. *Biochemistry* **1996**, *35*, 6366−6374.
(7) Lipinski, C.; Lombardo, F.; Dominy, B.; Feeney, P. Experimental and computational approaches to estimate solubility and permeability in drug discovery and development settings. *Adv. Drug Delivery Rev.* **1997**, *23*, 3−25.
(8) Wenlock, M.; Austin, R.; Barton, P.; Davis, A.; Leeson, P. A comparison of physiochemical property profiles of development and marketed oral drugs. *J. Med. Chem.* **2003**, *46*, 1250−1256.
(9) Hopkins, A.; Groom, C.; Alex, A. Ligand efficiency: a useful metric for lead selection. *Drug Discovery Today* **2004**, *9*, 430−431.
(10) Kuntz, I.; Chen, K.; Sharp, K.; Kollman, P. The maximal affinity of ligands. *Proc. Natl. Acad. Sci.* **1999**, *96*, 9997−10002.
(11) Popov, V.; Yee, W. A.; Anderson, A. Towards in silico lead optimization: scores from ensembles of protein:ligand conformations reliably correlate with biological activity *Proteins* **2006**, *66*, 375−387.
(12) Anderson, A. Two Crystal Structures of Dihydrofolate Reductase-Thymidylate Synthase from Cryptosporidium hominis Reveal Protein: Ligand Interactions Including a Structural Basis for Observed Antifolate *Resistance. Acta Crystallogr.* **2005**, *F61*, 258−262.
(13) O'Neil, R.; Lilien, R.; Donald, B.; Stroud, R.; Anderson, A. Phylogenetic classification of protozoa based on the structure of the linker domain in the bifunctional enzyme, dihydrofolate reductase-thymidylate synthase. *J. Biol. Chem.* **2003**, *278*, 52980−52987.
(14) Cody, V.; Luft, J.; Pangborn, W. Understanding the role of Leu22 variants in methotrexate resistance: comparison of wild-type and Leu22Arg, variant mouse and human dihydrofolate reductase ternary crystal complexes with methotrexate and NADPH. *Acta Crystallogr.* **2005**, *D61*, 147−155.
(15) Bolin, J.; Filman, D.; Matthews, D.; Hamlin, R.; Kraut, J. Crystal structures of Escherichia coli and Lactobacillus casei dihydrofolate reductase refined at 1.7 Å resolution. I. General features and binding of methotrexate. *J. Biol. Chem.* **1982**, *257*, 13650−13662.
(16) Champness, J.; Achari, A.; Ballantine, S.; Bryant, P.; Delves, C.; Stammers, D. The structure of Pneumocystis carinii Dihydrofolate Reductase to 1.9 Å Resolution. *Structure* **1994**, *2*, 915−924.
(17) Knighton, D.; Kan, C.; Howland, E.; Janson, C.; Hostomska, Z.; Welsh, K.; Matthews, D. Structure of and kinetic channeling in bifunctional dihydrofolate reductase-thymidylate synthase. *Nat. Struct. Biol.* **1994**, *1*, 186−194.
(18) Jones, M. L.; Baccanari, D. P.; Tansik, R. L.; Boytos, C. M.; Rudolph, S. K.; Kuyper, L. F. Inhibitors of dihydrofolate reductase: Design, synthesis and antimicrobial activities of 2,4-diamino-6-methyl-5-ethynylpyrimidines. *J. Heterocycl. Chem.* **1999**, *36* (1), 145−148.
(19) deSousa, P. T. The palladium-catalysed cross coupling reaction of acetylenic compounds with aryl halides and related compounds. *Quim. Nova* **1996**, *19* (4), 377−382.
(20) Muller, S.; Liepold, B.; Roth, G. J.; Bestmann, H. J. An improved one-pot procedure for the synthesis of alkynes from aldehydes. *Synlett* **1996**, *6*, 521−522.
(21) McMartin, C.; Bohacek, R. QXP: Powerful, rapid computer algorithms for structure-based drug design. *J. Comput.-Aided Mol. Des.* **1997**, *11*, 333−344.
(22) Jain, A., Surflex: Fully Automatic Flexible Molecular Docking Using a Molecular Similarity-Based Search Engine. *J. Med. Chem.* **2003**, *46*, 499−511.
(23) Jain, A. Ligand-Based Structural Hypotheses for Virtual Screening. *J. Med. Chem.* **2004**, *47*, 947−961.
(24) Ruppert, J.; Welch, W.; Jain, A. Automatic identification and representation of protein binding sites for molecular docking. *Protein Sci.* **1997**, *6*, 524−533.
(25) Welch, W.; Ruppert, J.; Jain, A. Hammerhead: fast, fully automated docking of flexible ligands to protein binding sites. *Chem. Biol.* **1996**, *3*, 449−462.
(26) Jain, A. Scoring noncovalent protein-ligand interactions: a continuous differentiable function tuned to compute binding affinities. *J. Comput.-Aided Mol. Des.* **1996**, *10*, 427−440.
(27) Danishefsky, S.; Harvey, D. A new approach to polypropionates: routes to subunits of monensin and tirandamycin. *J. Am. Chem. Soc.* **1985**, *107*, 6647−6652.
(28) Van Hijfte, L.; Kolb, M.; Witz, P. A practical procedure for the conversion of aldehydes to terminal alkynes by a one carbon homologation. *Tetrahedron Lett.* **1989**, *30*, 3655−3656.
(29) Bull, S.; Davies, S.; Key, M.; Nicholson, R.; Savory, E. Conformational control in the SuperQuat chiral auxiliary 5,5-dimethyl-4-isopropyloxazolidin-2-one induces the iso-propyl group to mimic a tert-butyl group. *Chem. Commun.* **2000**, *18*, 1721−1722.
(30) Rosowsky, A.; Forsch, R.; Queener, S. Further Studies on 2,4-Diamino-5-(2′,5′-disubstituted benzyl)pyrimidines as Potent and Selective Inhibitors of Dihydrofolate, Reductases from Three Major Opportunistic Pathogens of AIDS. *J. Med. Chem.* **2003**, *46*, 1726−1736.
(31) Rosowsky, A.; Fu, H.; Chan, D.; Queener, S., Synthesis of 2,4-Diamino-6-[2′-*O*-(ω-carboxyalkyl)oxydibenz[*b*,*f*]azepin-5-yl]methylpt eridines as Potent and Selective Inhibitors of *Pneumocystis carinii*, *Toxoplasma gondii*, and *Mycobacterium avium* Dihydrofolate Reductase. *J. Med. Chem.* **2004**, *47*, 2475−2485.
(32) Gangjee, A.; Devraj, R.; Queener, S. Synthesis and dihydrofolate reductase inhibitory activity of 2,4-diamino-5-deaza and 2,4-diamino-5,10-dideaza lipophilic antifolates. *J. Med. Chem.* **1997**, *40*, 470−478.
(33) Gangjee, A.; Adair, O.; Queener, S., Synthesis and biological evaluation of 2,4-diamino-6-(arylaminomethyl)pyrido[2,3-*d*]pyrimidines as inhibitors of *Pneumocystis carinii* and *Toxoplasma gondii* dihydrofolate reductase and as antiopportunistic infection and antitumor agents. *J. Med. Chem.* **2003**, *46*, 5074−5082.
(34) Rosowsky, A.; Chen, H.; Fu, H.; Queener, S. Synthesis of new 2,4-diaminopyrido[2,3-*d*]pyrimidine and 2,4-diaminopyrrolo[2,3-*d*]pyrimidine inhibitors of Pneumocystis carinii, Toxoplasma gondii and Mycobacterium avium dihydrofolate reductase. *Bioorg. Med. Chem.* **2003**, *11*, 59−67.

JM061027H